

PDF based seasonal changes in AgMERRA observations and GCM20 and RegCM4.3 projections over Pakistan Region

Burhan A[™], Athar H

Using recently published reanalysis dataset viz. Agriculture Modern-Era Retrospective Analysis for Research and Applications (AgMERRA), the present study has made use of Probability Density Functions (PDFs) to evaluate changes in mean, standard deviation, skewness and kurtosis of the two basic climate variables (mean temperature and mean precipitation) on seasonal basis in vulnerable and data sparse region of Pakistan. The historical (1980–1998), present and near future (2008–2025), and far future (2080–2098) climate datasets of a super high resolution GCM viz. GCM20 (20 Km horizontal resolution, A1B scenario), and of a high resolution RCM viz. RegCM4.3 (25 km horizontal resolution, RCP8.5 scenario) are used to construct the PDFs to assess probable changes in their statistics and to asses range of associated uncertainties. The AgMERRA dataset indicates that ninetieth percentile has increased (Δ DJF = 0.50°C) in 1990–1998 DJF daily mean temperature relative to 1980–1989 DJF daily mean temperature. For JJAS seasonal mean precipitation, the AgMERRA dataset shows relative decrease in the ninetieth percentile (Δ JJAS = -1.8 mm/day). The GCM20 (RegCM4.3) has shown a 2.1°C (4.7°C) warm shift in the ninetieth percentile of DJF daily mean temperature in 2008–2016 projection period relative to 1990–1998 baseline period. Moreover, the GCM20 (RegCM4.3) suggests a substantial JJAS mean precipitation increase of 9.0 mm/day (29.2 mm/day) in the ninetieth percentile for the 2008–2016 projection period.

INTRODUCTION

Uncertainty in climate predictability may be assessed by means of distributional moments such as mean, standard deviation, skewness and kurtosis (see, e.g., Wilks, 2011). The standard deviation apprehends the level of uncertainty in the climate change impacts, i.e., large values of it makes the tails of frequency distributions fatter resulting in an increased probability of extreme events. The skewness, owing to its characteristic ability to capture the degree of symmetry in the uncertainty, defines negative values as those under which the major fraction of the observations are greater than the mean. Reducing the negative skewness renders an increase in the probability of high–impact events relative to low–impact events. Large peaks (flat patterns) of the kurtosis exhibit uniform (dispersed) estimates about climate change impacts.

Climate variability and change may be identified by presenting a framework of time dependent Probability Density Functions (PDF) and by showing how the distribution of climatic values in the sample window make transitions over time (Larson, 2012; Kundu *et al.* 2015). Annual empirical anomaly PDFs have been computed over Saudi Arabia to assess variability in the observed daily mean temperature for a historical period of 1979–2008 (Athar, 2012). Michczynska and Pazdur (2004) computed PDFs to report on a statistical analysis based on a

Research and Development Division, Pakistan Meteorological Department, 44000, Islamabad, Pakistan;

©Correspondence to: Burhan Ahmad; Research and Development Division, Pakistan Meteorological Department, 44000, Islamabad, Pakistan; Email: burhanahmadkhan@gmail.com

broad collection of radiocarbon dates in order to reconstruct paleoclimate. The PDFs have been computed on seasonal basis to study variability in the observed daily mean temperatures of northern Saudi Arabia by making use of three decades out of a 31-year base period of 1978–2008 (Athar, 2013). Changes in the PDFs of daily gridded observational maximum and minimum temperatures over the globe have been investigated using two 30-year periods: 1951–1980 and 1981–2010 (Donat and Alexander, 2012). The last study points out a significant global shift of the variables towards higher values in the recent period in contrast to the older period with a relatively less significant and spatially heterogeneous changes in the variance.

Illustration of potential uncertainty in the projected climate change over the 21st century in the form of PDFs has broadly been desired for applications (Watterson, 2008). PDFs are to be interpreted as a signal of what outputs may be more conceivable than others, or as a move to convey uncertainty (Knutti, 2008). Robert (2014) studied the prospect of computing PDFs of daily precipitation through downscaling with plausible results of generating an adroit statistical model that could project future deviations of precipitation PDFs forced by General Circulation Model (GCM) simulations.

Global warming had been projected using time slice technique over a super high resolution GCM – GCM20 of 20-km horizontal resolution (Kusunoki *et al.*, 2006). The model simulated a pragmatic Baiu season (Japanese rainy season that occurs in boreal early summer over the Western North Pacific), northward seasonal drift of the Baiu rain band,

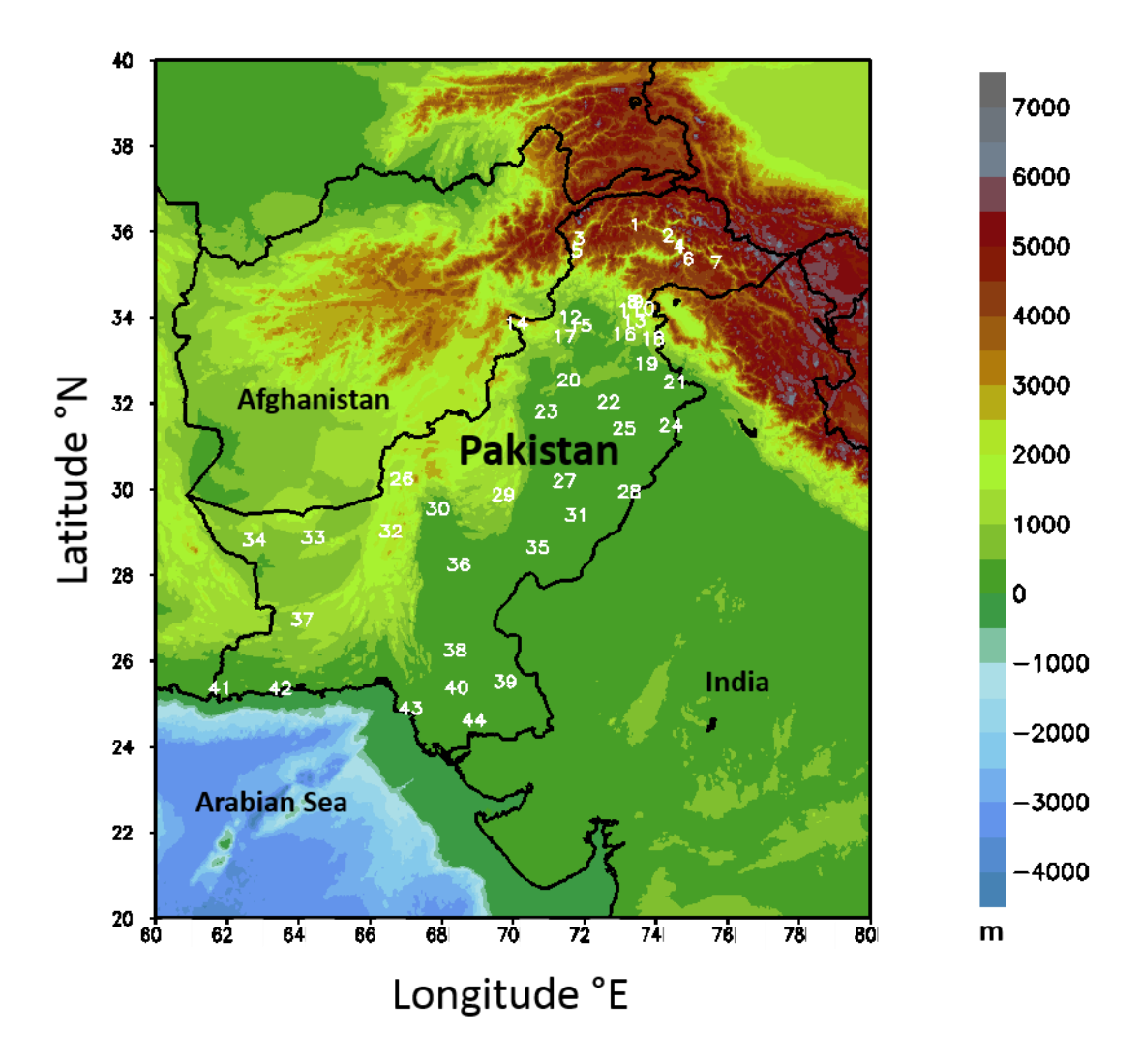


Figure 1 Relief map of study area. Elevation is represented in meters. Station network distribution of the study area is represented by corresponding serial numbers. See Table II for details of stations

its onset and withdrawal, intensity of precipitation and the geographic distribution of mean sea level pressure.

The Coordinated Regional Climate Downscaling Experiment (CORDEX) is a foundation drafted to integrate international attempts made on simulation of regional climate under domains that surround major land areas of the world (Ozturk *et al.*, 2012). The International Centre for Theoretical Physics (ICTP) based Regional Climate Model (RCM) named RegCM4.0, a contributor to the CORDEX project, has been widely brought to play owing to its enclosure of land surface, airsea flux schemes, planetary boundary layer, an assorted convection and tropical band configuration, under several CORDEX domains (Giorgi *et al.*, 2012).

Due to its latitudinal location (see Figure 1), climate of Pakistan remains temperate. Positioned between 20°N–40°N and 60°E–80°N, the country embodies an area of approximately 804,000 km²out of which the land covers an area of about 796,000 km² (see, e.g., Shamshad, 1988). Both seasonal and regional variations of meteorological variables are present in Pakistan. Day and night time temperature gradients are extremely large. Seasons in Pakistan are categorized into four classes; cold winter December-January-February (DJF), temperate spring March-April-May (MAM), warm and wet summer June-July-August-September (JJAS), and dry and cold autumn October-November (ON).

In summers, the temperature has tendency to hike up to 49°C or even higher over the southern parts of the country. Deserts of southern parts bear barrenness and dryness due to insufficient precipitation over the region. Since seasonal cycle over the country is strong, therefore seasonal analysis is chosen to be discussed in this paper.

DATA AND METHODOLOGY

Data

Baseline reanalysis dataset AgMERRA

In the present study, PDF based analysis of state of the art newly published Agricultural Modern Era Retrospective Analysis for Research and Applications (AgMERRA) datasets (Ruane *et al.*, 2014) for daily mean temperature and mean precipitation are carried out on country level in two 9 year batches during 1980–1998. This dataset has been developed from the previously established Modern Era Retrospective Analysis for Research and Applications (MERRA) by incorporating in situ and satellite sensed observational datasets for temperature, precipitation and other important meteorological variables. The AgMERRA introduces daily high resolution climate forcing datasets to study climate variability and climate change impacts in addition to their use in agriculture sector.

Table I Details of the three datasets used in the analysis

Dataset/Model	Available Period	Variables	Spatial Resolution	Time step	Scenario
AgMERRA	1981–2010	Temperature, Precipitation	25 km	Daily	_
GCM20	1979–1998	Temperature, Precipitation	20 km	Monthly	A1B
	2007–2025				
	2080–2098				
RegCM4.3	1970–2099	Temperature, Precipitation	25 km	3 hourly	RCP8.5

Table II Stations with their corresponding geographic locations and elevations. The stations are arranged in a latitudinal decreasing fashion

Sr. No.	Station Name	Latitude (°N)	Longitude (°E)	Elevation (m)	Sr. No.	Station Name	Latitude (°N)	Longitude (°E)	Elevation (m)
1	Gupis	36.17	73.40	4682	23	Dera Ismail Khan	31.82	70.92	174
2	Gilgit	35.92	74.33	1469	24	Lahore	31.50	74.40	216
3	Chitral	35.85	71.83	3049	25	Faisalabad	31.43	73.10	185
4	Bunji	35.67	74.63	1340	26	Quetta	30.25	66.88	1571
5	Drosh	35.57	71.78	1666	27	Multan	30.20	71.43	124
6	Astore	35.37	74.90	2945	28	Bahawalnagar	29.95	73.25	157
7	Skardu	35.30	75.68	2211	29	Barkhan	29.88	69.72	1114
8	Balakot	34.38	73.35	1188	30	Sibbi	29.55	67.88	139
9	Muzaffarabad	34.37	73.48	905	31	Bahawalpur	29.40	71.78	126
10	GhariDupatta	34.22	73.62	831	32	Kalat	29.03	66.58	2016
11	Kakul	34.18	73.25	1227	33	Dalbandin	28.88	64.40	848
12	Peshawar	34.02	71.58	323	34	Nokkundi	28.82	62.75	677
13	Murree	33.92	73.38	1658	35	Khanpur	28.65	70.68	92
14	Parachinar	33.87	70.08	1592	36	Jaccobabad	28.25	68.47	56
15	Cherat	33.82	71.88	1222	37	Panjgur	26.97	64.10	985
16	Islamabad	33.62	73.10	507	38	Nawabshah	26.25	68.37	29
17	Kohat	33.57	71.43	501	39	Chhor	25.52	69.78	3
18	Kotli	33.52	73.90	608	40	Hyderabad	25.38	68.42	24
19	Jhelum	32.93	73.72	232	41	Jiwani	25.37	61.80	15
20	Mianwali	32.55	71.55	208	42	Pasni	25.37	63.48	15
21	Sialkot	32.50	74.53	253	43	Karachi	24.90	67.13	26
22	Sargodha	32.05	72.67	191	44	Badin	24.63	68.90	10

Baseline and projected GCM20 dataset

Present research work has utilized the output from global 20-km mesh model, GCM20 – a collaborative development of Japan Meteorological Agency (JMA) and the Meteorological Research institute (MRI) Japan (see, e.g., Yatagai *et al.*, 2005; Kusunoki *et al.* 2006; Kitoh *et al.*, 2008; Kitoh *et al.*, 2009; Mizuta *et al.*, 2012 and references cited therein). The model has a linear Gaussian grid that triangularly truncates at 959 horizontal units. The model is based on operational numerical weather prediction model of JMA, and assimilates modifications in radiation and land surface processes. The available model simulation performed under A1B scenario is in three time slices: 1980–1998, 2007–2025, and 2080–2098 (Table I).

Baseline and projected RegCM4.3 CORDEX dataset

RegCM4.3 is the newly published, fourth generation development of ICTP based RCM (Giorgi et al., 2012). It is a hydrostatic model with

sigma based vertical coordinates, and is run on an Arakawa B-grid. The simulation period of the experimental design starts from 1st Jan 1970 to 31st Dec 2099, which captures both the reference and the projection periods. The initial and boundary conditions for the model came from CMIP5 based GFDL–ESM2M (RCP8.5) having 2.0°×2.5° spatial resolution (see, e.g., Ozturk *et al.*, 2012; Gu *et al.*, 2012; Franco *et al.*, 2013).

Methodology

Extraction of data at stations

For the 44 ground stations listed in Table II, extraction of daily mean temperature and mean precipitation from the AgMERRA dataset is performed (Burhan, 2016). To project statistics of the future climate, mean projected temperature and mean projected precipitation from the super high resolution GCM20 and from the state of the art RegCM4.3 are extracted over all ground stations (Table II).

The ground station selection includes a diverse meteorological context (urban, rural, snow-cover, agro-climate, latitudinal location, proximity to ocean, reach of monsoon (see, e.g., Wang, 2006) and westerly systems (see, e.g., Dimriet al., 2015) etc), and topography since these factors can result in much more variability in temperature and precipitation values than differences. Snow cover can have a major impact on mean temperature change (especially by its freeze and thaw process) in the vicinity of the selected ground station. Keeping in view of these dynamics, the ground station density in latitudes above 31°N (below 31°N) is 25(19). Zonally, seven ground stations are selected in the snow-covered glaciers of the Northern areas, three ground stations in the hills of Azad Jammu and Kashmir, eight ground stations in the hills and plains of Khyber Pakhtunkhwa, eleven ground stations in the plains of Punjab, six ground stations in the deserts and ocean bordering plains of Sindh, and nine ground stations in the barren hills and coastal line of Baluchistan.

Bias correction using delta method

Delta methods may be utilized under a large variation of methodologies(see, e.g., Minville et al., 2008; Tisseuil et al., 2010; Winkler et al., 2011; Chen et al., 2011) out of which "Linear Interpolation and Bias Correction (LIBC)" is chosen to serve as a bias correction tool for future projections under this study. LIBC is a merger of two techniques used by Wood et al., (2004) and Immerzeel et al., (2012). Under the LIBC stratagem, the AgMERRA datasets for mean temperature and mean precipitation were selected for the baseline period 1980-1998. Daily data series was first converted to monthly data series followed by corresponding conversion to climatology of the respective variable and to the climatology of the standard deviation of that variable. Afterwards, the dataset was regridded to a horizontal resolution of 0.22° for the complete baseline period 1975-2005. Afterwards, time sorting and area based tracing were performed for the GCM/RCM. The raw GCM/RCM data were then linearly interpolated (see, e.g. Wood et al., 2004; Fowler et al., 2007) to the grid description of the AgMERRA datasets. Afterwards correction factors were determined by the division of climatological values of observations to the climatological values of the reference GCM/RCM given by Eq. (1).

$$V_{\text{tuned}} = \frac{\overline{V_{obs}}}{\overline{V_{ref}}} \tag{1}$$

$$S_{\text{tuned}} = \frac{\overline{S_{obs}}}{\overline{S_{exe}}} \tag{2}$$

Where V_{tuned} is the adjusted factor for mean climate, $\overline{V_{obs}}$ is the observed climatology (i.e. climatology of the baseline dataset of AgMERRA) and $\overline{V_{ref}}$ is the reference climatology for the GCM/RCM baseline. S_{tuned} is the signal to noise ratio obtained by dividing the square root of the variance of the monthly observed dataset $\overline{S_{obs}}$ with the square root of the variance of the monthly GCM/RCM reference $\overline{S_{ref}}$.

The revised climate variables are computed by multiplying signal to noise ratio of the corresponding month given by Eq. (2) with the deviation between future GCM/RCM month and climatology of that month given by Eq. (3). Afterwards result is added to the product of adjusted factor and the respective climatology of that particular month given by Eq. (4). Repeating the same procedure with each month of the future GCM/RCM data, we obtain the revised monthly GCM/RCM values for both mean temperature and mean precipitation variables. The mathematical scheme followed under this method is

$$E_s = \left(V_{proj} - \overline{V_{ref}}\right) \cdot S_{tuned} \tag{3}$$

$$E_{proj} = E_s + \left(\overline{V_{ref}} \cdot V_{tuned}\right) \tag{4}$$

Where E_s is the signal enhanced or signal dampened for a particular projection month, V_{proj} is the particular projected month that needs correction and S_{tuned} is same as described earlier. E_{proj} is the bias corrected climatic variable for the particular month, $\overline{V_{ref}}$ and V_{tuned} are same as defined earlier.

Temporal aggregation and disaggregation

Temporal disaggregation of GCM20 (from monthly to daily) and temporal aggregation of RegCM4.3 (from 3 hourly to daily) had been performed to synchronize the temporal resolutions of the models' output into daily format (Salathe, 2004). In temporal disaggregation technique, diurnal variations from a projection month are imposed upon all grids of the extracted monthly values. To disaggregate mean precipitation variable, daily climatology of the AgMERRA data is acquired for each grid and then calibrated in a model such that the monthly mean precipitation is equal to the model extracted mean precipitation for the corrected month. For mean temperature, the temporal disaggregation is executed by employing the same methodology, except for that the calibration was multiplicative rather than additive.

Kernel smoothing density and PDFs

The kernel smoothing density yields a probability density estimate for the sample in the variable vector (see, e.g., Wand and Jones, 1995). The estimate makes its foundations on a normal kernel function. The PDFs of both mean temperature and mean precipitation were constructed using kernel smoothing density function:

$$g = ksdensity(y, vJ, k) = \frac{1}{n} \sum_{i=1}^{n} \frac{1}{\sqrt{2\pi}} \cdot \frac{1}{k} \cdot e^{\frac{-(y-vJ_i)^2}{2k^2}}$$
 (5)

Where y is the value to be computed for density, vJ is the distributed sample used as kernel median, k (> 0) is the bandwidth used as scale of the kernel, and g is the required probability density estimate.

Seasonal analysis over Pakistan is performed for daily mean temperature and mean precipitation for baseline period (1981–1998) and projected periods (2008–2025, 2081–2098) by constructing their PDFs in order to identify possible climate change signatures in the region. Each period is divided into two halves. Daily mean precipitation is considered for wet days only (mean precipitation > 0.0 mm) such that it also includes days with trace amount of precipitation. Tenth and ninetieth percentiles (P10 and P90) for the first baseline period are plotted to assess decadal changes in extreme cold and extreme warm daily mean temperature frequencies.

RESULTS AND DISCUSSION

AgMERRA based PDFs

Figure 2 displays PDFs of the baseline period constructed from AgMERRA's daily mean temperature. In the DJF, the shapes of the PDFs are bimodal with high values of kurtoses where highest frequencies occur at –8°C and 14°C for the first half (1981–1989) and at –7°C and 15°C for the second half (1990–1998). The bimodality in the DJF is due to simultaneous recurrence of relatively warm mean temperatures in the south and relatively cold mean temperatures in the north of the country. In the DJF, above P90, the relative frequency of extreme warm mean temperatures in the second half continue to remain 0.5°C above that in first half. For the first half, the P10 in MAM lies at

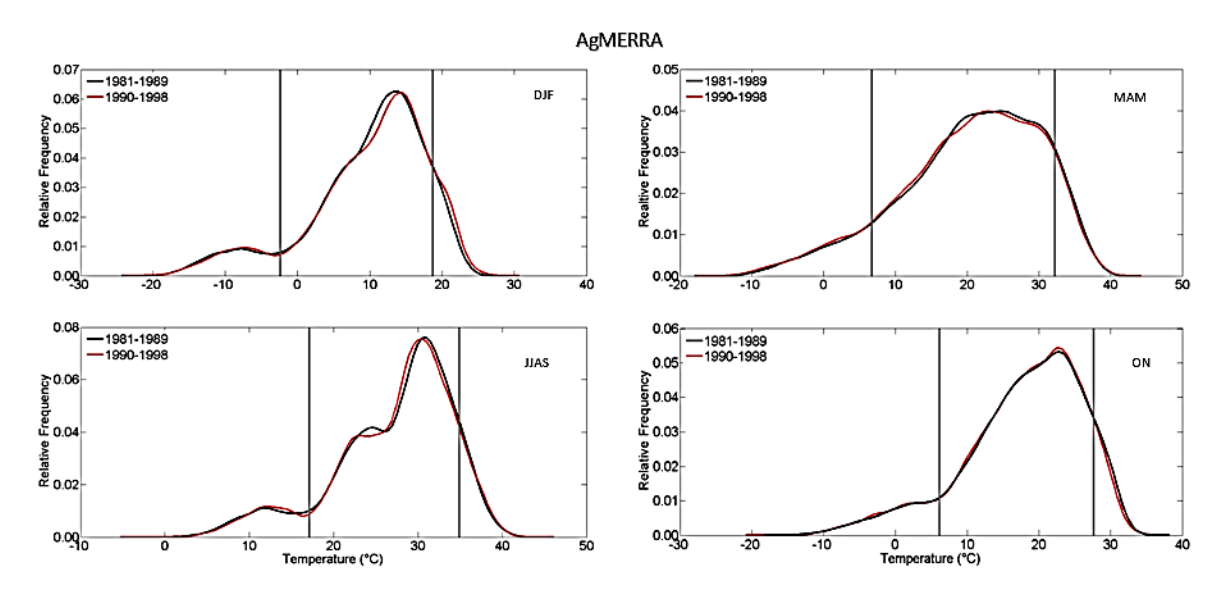


Figure 2 AgMERRA based seasonal PDFs of daily mean temperatures (°C) across Pakistan during the baseline period (1981–1998). Grey left (right) vertical lines represent tenth (ninetieth) percentiles of the first baseline half period (1981–1989)

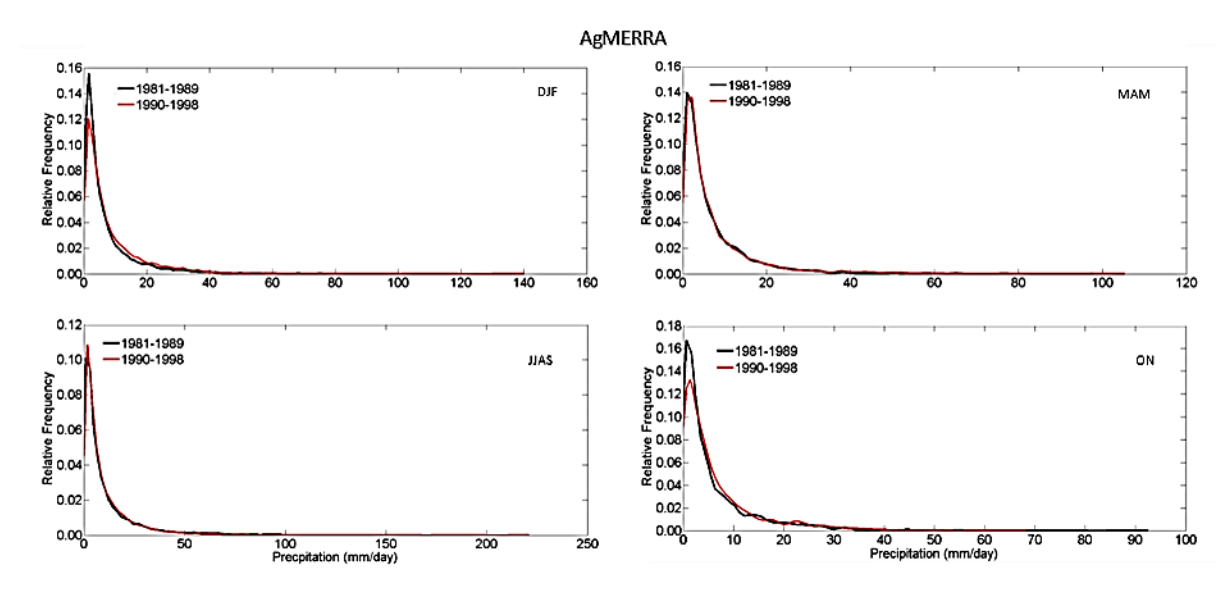


Figure 3 AgMERRA based seasonal PDFs of daily mean precipitation (mm/day) across Pakistan during the baseline period (1981–1998)

7°C, whereas the P90 lies at 32.5°C. Relative occurrence of the two baseline periods do not diverge significantly for both below P10 and above P90 in the MAM. However the probability of occurrence of the mean temperature range (18°C to 32°C) for the second half remains below the mean temperature range for the first half in the same season. The probability of occurrence of the second half remains above the probability of occurrence of the first half for JJAS mean temperature values that are below P10. This suggests that relative probability in the frequency of cold days has increased in the second half with respect to the first half. The probability of occurrence of JJAS mean temperature of second half remains below the probability of occurrence of JJAS mean temperature of the first half for the mean range between P10 and P90.

Figure 3 is the kernel smoothed daily mean precipitation PDFs of the baseline period constructed from the AgMERRA daily dataset. Probability of occurrence of the 3 mm/day DJF mean precipitation gets the highest peaks in both the first and the second halves. The relative frequency of the highest peak attained by the second half is smaller (relative frequency=0.12) than the highest peak attained by the first half (relative frequency=0.16). The result suggests a probability decrease in the DJF daily mean precipitation occurrence in the later half than that in the former half. However the probability of occurrence of relatively extreme DJF mean precipitation events (10 mm/day to 30 mm/day) has increased in the later half than that in the former half. Probability occurrences of both halves in MAM have remained unchanged. Maximum probability of occurrence of JJAS daily mean precipitation occurs at 4 mm/day with relative frequency=0.11 for both halves. Maximum relative frequency of the ON daily mean precipitation for the first half occurs at 0.17 and for the second half occurs at 0.13. This indicates a relative probability decrease in the frequency of 1.5 mm/day ON mean precipitation in the later half as compared to the former half. There is a relative frequency increase in the second baseline period

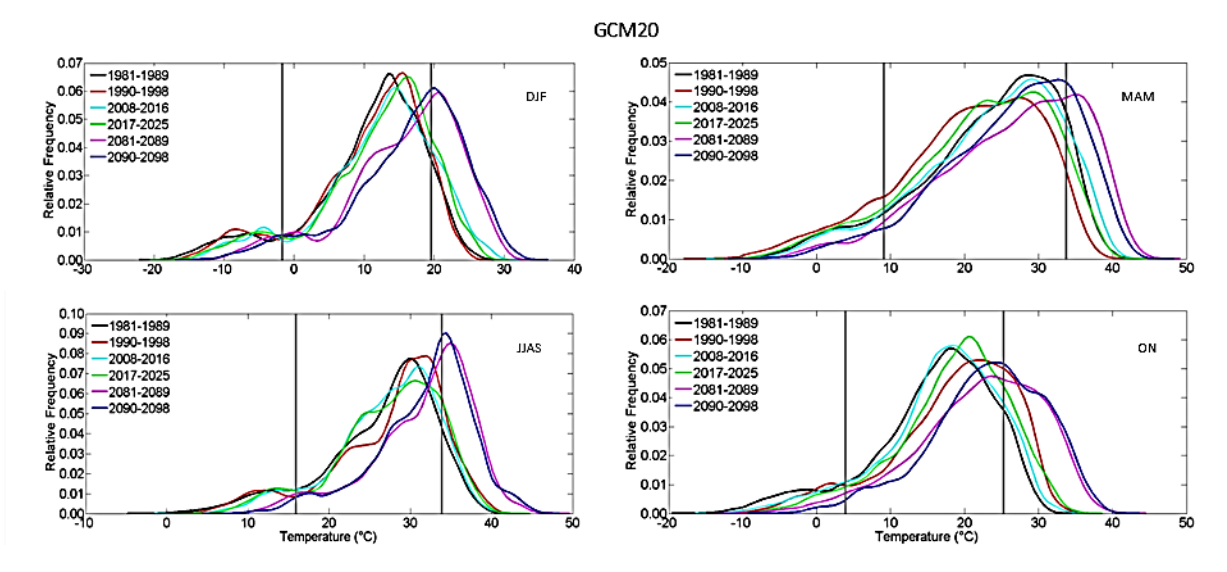


Figure 4 Same as in Figure 2 except for GCM20, including the near and far future projection periods

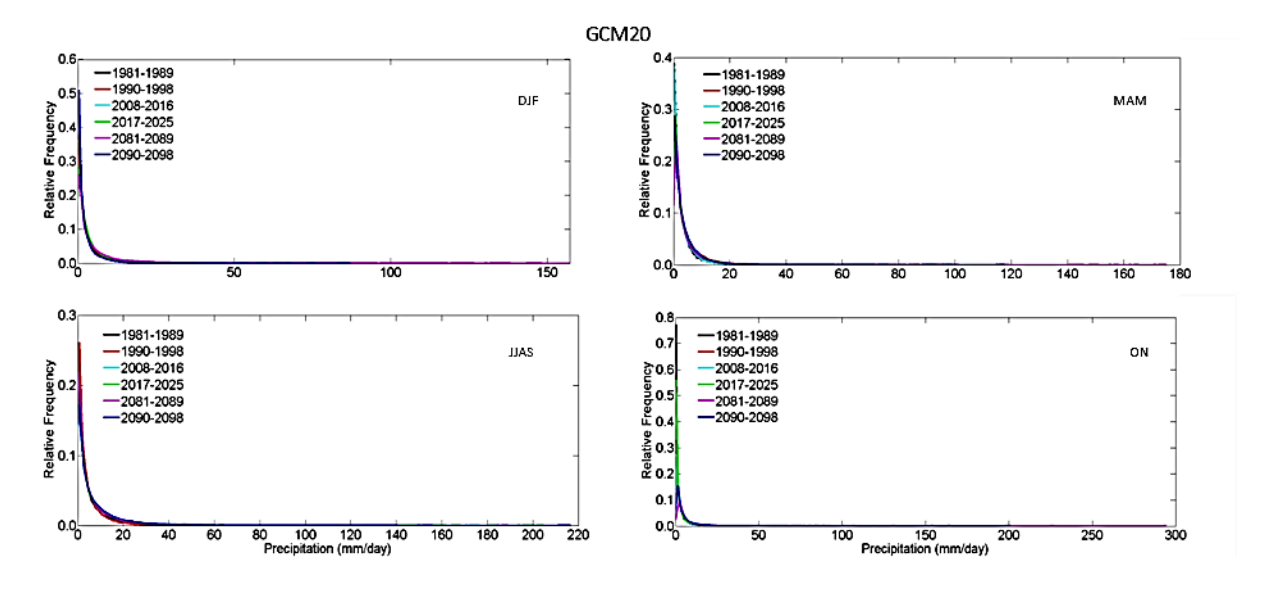


Figure 5 Same as in Figure 3 except for GCM20, including the near and far future projection periods

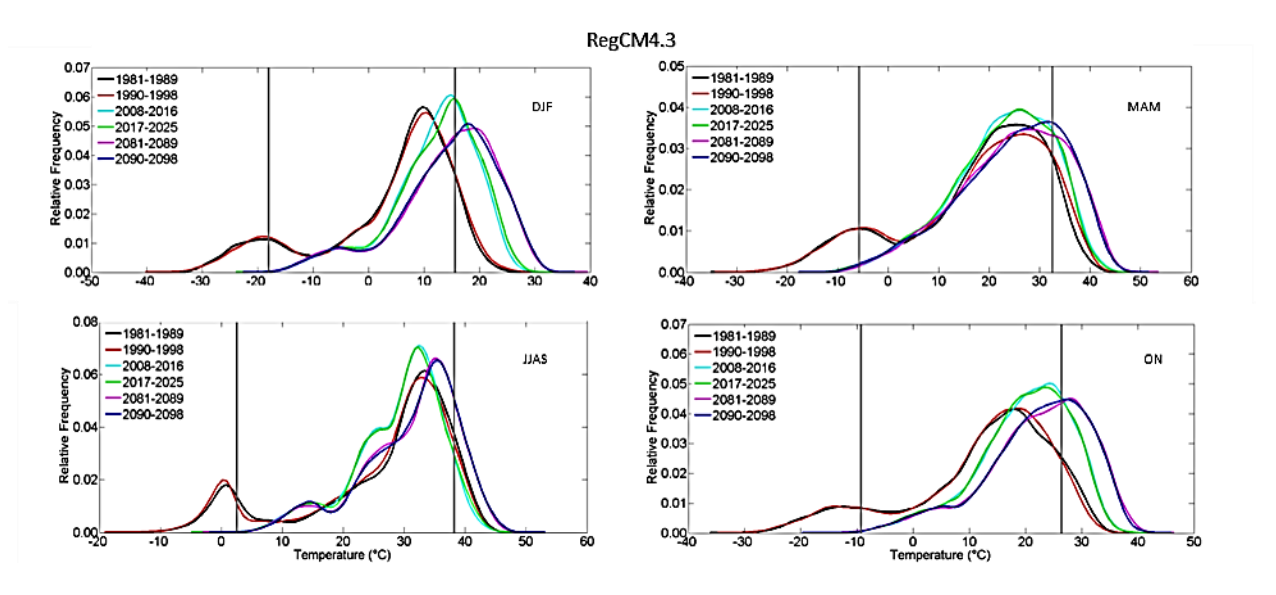


Figure 6 Same as in figure 4 except for RegCM4.3

when the probability occurrence of the mean daily ON mean precipitation ranges from 10 mm/day to 15 mm/day. The result signifies that in transition from summer monsoon to winter season, the occurrence of 10 mm/day to 15 mm/day mean precipitation events have increased in the second half of the ON in Pakistan.

GCM20 based PDFs

Figure 4 is representation of kernel smoothed PDFs constructed from delta correctedGCM20 daily mean temperature data using Eq. (3) to Eq. (5). Cold days in DJF for the present (2008-2016) and the immediate future (2017-2025) period are more negatively skewed than those in the first and the second halves of the baseline period. A probable 3°C warm shift in DJF daily mean temperature with a galvanized relative frequency change from 0.060 towards 0.065 is also seen. Furthermore, it is seen that the probability of occurrence of DJF warm days in the immediate future decreases as compared to the present period and increases as compared to the two baseline half periods of the past. The far-future (2081-2089 and 2090-2098) daily mean temperature PDFs for the DJF exhibit higher values of skewnesses and smaller values of kurtoses than those in the immediate future period and in the two baseline half periods. A comparison of MAM daily mean temperature PDF for the present period with that of the immediate future PDF indicates that a relative occurrence of the days in the immediate future with warm daily mean temperatures is likely to increase from 0.040 to 0.043 (for daily mean temperature of 23°C) and is likely to decrease from 0.047 to 0.042 (for daily mean temperature of 29°C). The relative frequencies of MAM cold days in both the far future periods are lower than those of all the previous time periods. This suggests smaller number of cold days and large number of relatively warm days to recur in both the MAM far-future periods. The occurrence of mean of the JJAS daily mean temperature drops down from 0.074 to 0.065 (mean temperature= 30°C) in the immediate future, as compared to the present period. The result is a relative cooling in the moderate mean temperature range and a relative warming in the cooler mean temperature range in the present and the immediate future period of JJAS. As compared to the present period, the first future highest recurrence has a warm shift of 4°C (from 13°C to 17°C), the second has a warm shift of 3°C (from 26°C to 29°C), and the third has a warm shift of 5°C (from 30°C to 35°C) in the JJAS. Relative negative skewness and kurtosis of the first far-future period is smaller than those in the second far-future period, which suggests higher occurrences of warm ON days and lower occurrences of cold ON days in the last decade of the 21st century as compared to those in the second-last decade of the 21st century.

Figure 5 is a representation of daily mean precipitation PDFs for the two baseline and the four projected periods, constructed from the delta corrected mean precipitation data of GCM20 using Eq. (3) to Eq. (5). Relative occurrences of 5 mm/day to 35 mm/day mean precipitation events in the present and the immediate future period are higher than those in the first baseline half period, though they are lower than those in the first far-future half period in DJF. There is a probability increase in the occurrence of 10 mm/day to 30 mm/day mean precipitation events in the immediate and far-future periods as compared to the first MAM baseline half period, and a decrease as compared to the second MAM baseline half period. Relative occurrences of both present and immediate future periods' JJAS 5 mm/day to 45 mm/day mean precipitation events are higher than those of the two baseline half periods. The relative frequencies of 5 mm/day to 30 mm/day mean precipitation events in the present and immediate future periods overlap with those in the two baseline periods, yet the relative frequencies of 5 mm/day to 30 mm/day

mean precipitation events in the two far-future periods increase as compared to the overlapped baseline and projected periods of the ON.

RegCM4.3 based PDFs

Figure 6 displays kernel smoothed daily mean temperature PDFs for the two baseline halves and the four projected periods, constructed from the delta corrected mean temperature data of RegCM4.3 using Eq. (3) to Eq. (5). Relative skewnesses and kurtoses of the present and the immediate future DJF periods are larger than those of the two baseline half periods. Moreover, relative skewnesses of the far-future periods are higher and the corresponding relative kurtoses are lower than those of the two baseline halves, the present, and the immediate future DJF periods. The results suggest a warm shift in the mean of the projected periods' PDFs, which further indicates a relative decrease in the number of DJF cold days and a relative increase in the number of DJF warm days. Relative negative skewnesses of present, immediate future, and both the farfuture half periods are higher than those of the two baseline MAM half periods. This suggests a relative warm shift in the mean of the projected MAM mean temperature PDFs. Furthermore, kurtoses of the present and the immediate future periods are higher than those of the two baseline half periods, suggesting warm MAM days to recur with higher frequencies in the projected periods. Relative occurrences of 25°C mean temperature in JJAS has increased from 0.02 to 0.04 in the present and the immediate future periods as compared to those in the two baseline half periods. Furthermore, relative occurrences of 33°C in JJAS has increased from 0.06 to 0.07 in the present and the immediate future periods as compared to that in the two baseline half periods. The results suggest convergence of both warm and cold JJAS mean temperatures towards mean JJAS temperature, with highest recurrence at 25°C and 33°C, in the present and immediate future period, as compared to the two baseline half periods. Relative occurrences of JJAS warm days (above the P10 of the first baseline half period) have significantly increased, while relative occurrences of JJAS cold days (below the P10 of the first baseline half period) have significantly decreased in the farfuture half periods as compared to those in the baseline half periods. Higher negative skewnesses of the far-future PDFs have rendered a warm shift (from 33°C to 36°C) in the mean of the far-future JJAS mean temperature PDFs as compared to those of the two baseline half periods. Higher values of negative skewnesses and kurtoses of the ON mean temperature PDFs in the present and the immediate future periods have rendered a warm shift in the PDFs' mean, and a higher relative frequencies of ON warm days to recur in the immediate future period, as compared to those in the two baseline half periods.

Figure 7 displays mean precipitation PDFs for the two baselines half periods and the four projected time periods, based on the delta corrected RegCM4.3 data output using Eq. (3) to Eq. (5). Occurrences of 5 mm/day to 40 mm/day DJF mean precipitation events are higher in the projected half periods as compared to those in the baseline half periods. Relative occurrence of <5 mm/day mean precipitation events in MAM is highest for the first baseline half period, is second highest for the second baseline half period, and gets lower with a significant drop for the projection periods. Mean precipitation occurrences of 5 mm/day to 40 mm/day display a significant increase in its recurrence in the projected half periods as compared to the baseline half periods of the MAM. Occurrence of 5 mm/day to 20 mm/day mean precipitation occurrences is highest for the far-future periods and of 21 mm/day to 40 mm/day is highest for the immediate future half periods in the MAM. The analysis suggest a relatively high occurrences of higher magnitude mean precipitation events in the immediate and the two far-future half periods

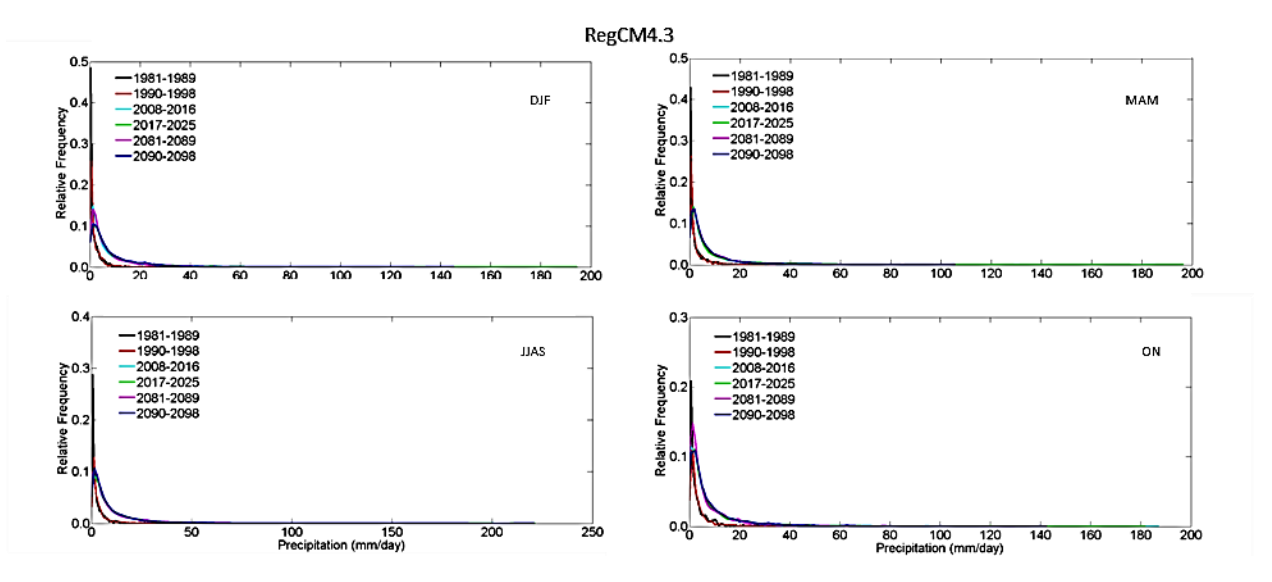


Figure 7 Same as in Figure 5 except for RegCM4.3

Table III Measures of dispersion in AgMERRA temperature and their seasonal changes during the two baseline half periods

Time Period	Statistic	DJF	MAM	JJAS	ON
1981–1989					
	P10 (°C)	-2.4	6.7	17.1	6.1
	P50 (°C)	11.5	21.8	28.9	19.3
	P90 (°C)	18.7	32.2	34.9	27.6
	Mean (°C)	9.7	20.5	27.2	17.9
	SD (°C)	8.3	9.8	7.1	8.4
	Skewness	-1.0	-0.6	-0.9	-0.9
	Kurtosis	3.8	2.9	3.6	3.5
1990–1998					
	P10 (°C)	-2.4	6.2	17.1	6.0
	P50 (°C)	11.8	21.5	28.8	19.1
	P90 (°C)	19.2	32.1	34.9	27.2
	Mean (°C)	10.0	20.2	27.2	17.8
	SD (°C)	8.4	9.9	7.1	8.4
	Skewness	-1.0	-0.6	-0.9	-0.9
	Kurtosis	3.7	2.9	3.5	3.5
1990–1998 minus 1981–1989					
	Δ P10 (°C)	0.0	-0.5	0.0	-0.1
	Δ P50 (°C)	0.3	-0.3	-0.1	-0.2
	Δ P90 (°C)	0.5	-0.1	0.0	-0.4
	Δ Mean (°C)	0.2	-0.3	0.0	-0.1
	Δ SD (°C)	0.1	0.1	-0.1	-0.1
	ΔSkewness	0.0	0.0	0.0	0.0
	∆ Kurtosis	-0.1	0.0	-0.1	0.0

of the MAM. Probability of occurrences of 5 mm/day to 55 mm/day mean precipitation events is highest for the projected periods, as compared to those of the baseline periods in JJAS. Relative occurrences of 5 mm/day to 40 mm/day ON mean precipitation events are higher in the projected half periods as compared to those in the baseline half periods.

Quantitative changes in measures of climatic variables dispersion

Table III represents changes in multiple measures of dispersion of the AgMERRA seasonal mean temperature between the two baseline half periods. The P10 of both transitional seasons (MAM and ON) have decreased (Δ MAM = -0.50°C and Δ ON = -0.10°C) in the second baseline half period, which indicates a relative decrease in cold spring

and autumn days recurrence in the second baseline half period. Fiftieth percentile (P50) of DJF has increased and that of JJAS, MAM and ON has decreased in the second baseline half period, which suggests median temperature increase (Δ DJF = 0.30°C) in the DJF and median temperature decrease in the remaining seasons of the second baseline half period as compared to the first baseline half period. The P90 of DJF has increased (Δ DJF = 0.50°C), whereas that of MAM and ON has decreased in the second baseline half period. Mean temperature of DJF has increased (Δ DJF = 0.25°C) while that of the remaining seasons have decreased in the second baseline half period. One sigma standard deviations (SD) of DJF and MAM have increased while those of JJAS and ON have decreased in the second baseline half period, suggesting relatively larger mean temperature departures from the mean in DJF and

Table IV Measures of dispersion in AgMERRA precipitation and their seasonal changes during the two baseline half periods

Time Period	Statistic	DJF	MAM	JJAS	ON
1981–1989					
	P10 (mm/day)	8.0	0.8	1.0	0.4
	P50 (mm/day)	3.6	3.9	5.2	2.8
	P90 (mm/day)	17.7	17.0	27.4	15.6
	Mean (mm/day)	7.1	7.0	10.9	5.9
	SD (mm/day)	9.3	8.6	15.3	8.1
	Skewness	3.1	3.0	3.2	3.3
	Kurtosis	17.6	16.6	17.2	21.0
1990–1998					
	P10 (mm/day)	1.0	1.0	1.1	0.5
	P50 (mm/day)	4.7	4.1	5.4	3.6
	P90 (mm/day)	21.8	18.9	25.6	17.5
	Mean (mm/day)	8.8	8.0	10.6	6.6
	SD (mm/day)	11.8	10.8	14.9	8.2
	Skewness	3.8	3.2	4.1	2.4
	Kurtosis	24.8	16.0	32.1	10.6
1990–1998 minus 1981–1989					
	Δ P10 (mm/day)	0.2	0.2	0.1	0.1
	Δ P50 (mm/day)	1.1	0.2	0.2	0.8
	Δ P90 (mm/day)	4.1	1.9	-1.8	1.9
	Δ Mean (mm/day)	1.7	1.0	-0.3	0.7
	Δ SD (mm/day)	2.5	2.1	-0.4	0.1
	ΔSkewness	0.6	0.2	1.0	-0.9
	Δ Kurtosis	7.2	-0.7	14.9	-10.4

Table V Changes in simulated and projected measures of dispersion in GCM20 seasonal temperature

Time Period	Statistic	DJF	MAM	JJAS	ON
2008-2016 minus 19	81-1989 (2008-2016 mir	nus 1990–1998)			
	Δ P10 (°C)	2.1 (2.5)	0.7 (3.4)	2.1 (1.2)	2 (-0.5)
	Δ P50 (°C)	1 (0.9)	0.1 (3.4)	0.1 (-1.2)	0.8 (-2.0)
	Δ P90 (°C)	1.9 (2.1)	0.7 (2.7)	0.4 (-0.6)	0.8 (-1.7)
	Δ Mean (°C)	1.4 (1.4)	0.4 (3.1)	0.7 (-0.4)	1.1 (-1.6)
	ΔSD (°C)	-0.1 (0.1)	0 (-0.2)	-0.7 (-0.8)	-0.5 (-0.4)
	∆ Skewness	0.2 (0.2)	0.1 (0)	0.2 (0.2)	0.1 (0)
	∆ Kurtosis	-0.4 (-0.1)	-0.1 (0)	-0.3 (-0.1)	-0.1 (0.3)
2017–2025 minus 19	81-1989 (2017-2025 mir	nus 1990–1998)			
	Δ P10 (°C)	1.6 (2)	-0.8 (1.8)	2.1 (1.1)	4 (1.6)
	Δ P50 (°C)	1.4 (1.2)	-1.5 (1.8)	0.4 (-0.9)	2.3 (-0.5)
	Δ P90 (°C)	1.4 (1.5)	-0.4 (1.6)	0.9 (-0.1)	2.1 (-0.5)
	Δ Mean (°C)	1.4 (1.4)	-1.0 (1.8)	1 (-0.1)	2.7 (-0.1)
	ΔSD (°C)	-0.2 (0)	0.1 (-0.1)	-0.5 (-0.6)	-0.8 (-0.7)
	∆ Skewness	0.1 (0)	0.1 (0)	0.2 (0.2)	0.2 (0.2)
	∆ Kurtosis	-0.2 (0.1)	-0.2 (0)	-0.5 (-0.3)	-0.3 (0.1)
2081–2089 minus 19	81-1989 (2081-2089 mir	nus 1990–1998)			
	Δ P10 (°C)	6.1 (6.5)	3.5 (6.2)	6.4 (5.5)	6.4 (3.9)
	Δ P50 (°C)	4.9 (4.8)	3.1 (6.3)	4.9 (3.7)	5.8 (3.1)
	Δ P90 (°C)	5.3 (5.4)	4.1 (6.1)	4.4 (3.4)	6.8 (4.2)
	Δ Mean (°C)	5.1 (5.1)	3.4 (6.1)	5.2 (4.1)	6.2 (3.5)
	ΔSD (°C)	-0.2 (-0.1)	0.2 (0.1)	-0.7 (-0.8)	0.1 (0.2)
	∆ Skewness	0.2 (0.2)	0.1 (0)	0.1 (0.1)	0.3 (0.2)
	∆ Kurtosis	-0.4 (-0.2)	-0.2 (0)	-0.1 (0)	-0.5 (-0.2)
2090–2098 minus 19	81-1989 (2090-2098 mir	nus 1990–1998)			
	Δ P10 (°C)	6.4 (6.8)	4.4 (7.1)	7.4 (6.4)	8.8 (6.3)
	Δ P50 (°C)	5.5 (5.4)	2.7 (6)	4.8 (3.6)	6.5 (3.7)
	Δ P90 (°C)	5.9 (6)	2.9 (4.9)	4.4 (3.4)	7.4 (4.8)
	Δ Mean (°C)	5.8 (5.8)	3.1 (5.8)	5.3 (4.2)	7.3 (4.6)
	Δ SD (°C)	-0.2 (0)	-0.4 (-0.6)	-1.0 (-1.1)	-0.6 (-0.5)
	∆ Skewness	0.2 (0.1)	0.1 (-0.1)	0.2 (0.2)	0.4 (0.3)
	∆ Kurtosis	-0.3 (0)	0 (0.2)	0 (0.1)	-0.6 (-0.3)

MAM and relatively smaller mean temperature departures from the mean in JJAS and ON. Relative skewness displays a decrease in the second baseline half period of DJF, MAM and JJAS, while it displays an

increase (Δ ON = 0.01) in the second baseline half period during the ON.

Table IV represents changes in various measures of dispersion in the AgMERRA mean precipitation between the two baseline half periods. There is a significant increase in the measures of dispersion for the DJF during the second baseline half period. All measures of dispersion in the MAM display an increase in the second baseline half period (except for Δ kurtosis MAM = -0.68 with a negative change) suggesting that a relative increase in P10, P50, P90 and mean precipitation has occurred with relatively higher deviations from the mean in the second baseline half period. There is an increase in the P10 and the P50 mean precipitation occurrences with higher values of skewness and kurtosis in the second baseline half period during JJAS. However, there is a relative decrease in the P90 (Δ JJAS = -1.8 mm/day) and the mean (Δ JJAS = -0.28 mm/day) JJAS mean precipitation with smaller disperse in the second baseline half period of JJAS. The P10, the P50, the P90 and the mean precipitation in ON has increased with decreased magnitude of relative skewness and kurtosis (Δ Kurtosis ON = -10.38 and Δ Skewness ON = -0.86), suggesting smaller relative occurrences of trace and higher relative occurrences of P10, P50 and P90 mean precipitation events in the second baseline half period of ON.

Table V represents changes in various measures of dispersion of GCM20 mean temperature data on seasonal basis for the baseline and the projected periods. Positive changes in kurtoses of GCM20 mean temperature are observed in MAM and ON for the present period minus the second baseline half period (Δ MAM = 0.04 and Δ ON = 0.27), in DJF and ON of the immediate future period minus the second baseline half period (\triangle DJF = 0.09 and \triangle ON = 0.06), in JJAS of the first farfuture period minus the second baseline half period (Δ JJAS = 0.02), in MAM and JJAS of the second far-future half period minus the second baseline half period (Δ MAM = 0.17 and Δ JJAS = 0.1), and in the MAM of the second far-future period minus the first baseline half period (Δ MAM = 0.01). Nearly all time-scales display positive changes in the recurrence of P10, with the exception in ON of present period minus second baseline period, and in MAM of immediate future period minus first baseline half period (Δ MAM = -0.17°C). This suggests that a relative decrease in occurrence of cold ON days has occurred in the present period in contrast with the second baseline half period, and that a relative decrease in occurrence of cold MAM days is expected in the immediate future in relevance with the first baseline half period. There is a P50, a P90 and a mean temperature decrease in the JJAS and ON of the present period minus the second baseline half period, in the JJAS and ON of immediate future minus the second baseline half period, and in the MAM of the immediate future period minus the first baseline half period. Simultaneous positive changes in mean and SD is noticed in DJF of the present period minus the second baseline half period, in MAM and ON of the first far-future period minus the second baseline half period, and in the MAM and ON of the first far-future period minus the first baseline period. These simultaneous positive changes in the mean and the SD are precursor to occurrence of extreme events (heat waves and cold waves), and are projected in the DJF of the present period, as well as in the MAM and ON of the first far-future half period.

Table VI represents changes in multiple measures of dispersion of GCM20 mean precipitation output for the projected periods along with the baseline period. Simultaneous negative changes in the kurtoses and the skewnesses, with simultaneous positive changes in the P90, the mean and the SD are noticed in JJAS of the present period minus the first baseline period, in the ON of the immediate future period minus the second baseline half period, in the MAM of the immediate future period minus the first baseline half period, and in the MAM of the second farfuture period minus the first baseline half period. Simultaneous positive

changes in the P90, the mean and the SD are an indication of occurrence of extreme precipitation events that are likely to cause floods with potential to damage lives and properties (see, e.g., Rasmussen *et al.*, 2015).

Table VII represents changes in multiple measures of dispersion of RegCM4.3 mean temperature output for the projected periods along with the baseline periods. With reference to both the baseline half periods, the DJF displayed highest positive changes in its kurtoses in all the projected periods. However, significant positive changes in DJF kurtoses are noticed in the present period minus the second baseline half period (Δ DJF = 0.50), in the present period minus the first baseline period (\triangle DJF = 0.50), in the immediate future period minus the second baseline half period (Δ DJF = 0.40), and in the immediate future minus the first baseline half period (Δ DJF = 0.40). The relative corresponding changes in the skewnesses, the P90, and the mean temperature in the DJF are also positive indicating warm shift in the mean DJF daily mean temperature with a relatively higher occurrence of warm DJF days in the immediate future. Amongst all the percentile changes in the DJF, P10 (as well as their corresponding kurtoses) has the highest positive changes in both the immediate and the far-future periods. This means that there is a large warm shift in the DJF cold days owing to which the frequency of DJF warm days is likely to recur more than the frequency of DJF cold days in the immediate and far future periods. Moreover, there is a relative decrease in the P90 and a relative corresponding increase in the P10 of the JJAS in both the present and the immediate future periods. This suggests a convergence of warm JJAS days towards the mean JJAS daily mean temperature (a relative cooling in warm JJAS days), and a convergence of cold JJAS days towards the mean JJAS daily mean temperature (a relative warming in cold JJAS days) in the present and immediate future periods.

Table VIII represents changes in measures of dispersion of RegCM4.3 seasonal mean precipitation for the projected periods along with the baseline period. Highest changes in P10 are in DJF and JJAS of the second far-future half period (Δ DJF = Δ JJAS = 0.9 mm/day). The P50 displays highest changes in the JJAS of both the present period and the immediate future period (Δ JJAS = 5.3 mm/day for both the periods). The P90, the mean precipitation and the SD of RegCM4.3 display highest changes in JJAS of the present period minus the second baseline half period (Δ JJAS P90 = 29.2 mm/day, Δ JJAS Mean = 11.1mm/day, and \triangle JJAS SD = 15.6 mm/day), and in the JJAS of the present period minus the first baseline half period (Δ P90 = 29.9 mm/day and Δ Mean = 11.5 mm/day, Δ SD = 16.7 mm/day). The results indicate a substantial increase in the mean JJAS daily mean precipitation departures in the present and the immediate future periods, owing to which the probability of precipitation borne disasters (like flash flooding, land sliding etc.) is likely to increase in the immediate future.

SUMMARY AND CONCLUSIONS

AgMERRA displays that P90 had increased (Δ DJF = 0.50°C) owing to which the relative frequency of extreme warm mean temperatures in 1990–1998 DJF continued to remain 0.5°C higher than its previous decade. GCM20 suggests 3°C warm shift in DJF daily mean temperature in 2008–2025 projection period. RegCM4.3 also suggests a warm shift in the mean of its PDFs, which indicates a relative decrease in the number of DJF cold days and a relative increase in the number of DJF warm days in 2008–2025 and 2080–2098 projection periods. For the MAM, AgMERRA displays that P10 had decreased (Δ MAM = -0.50°C) in the 1990–1998 baseline period. GCM20 suggests a P10 frequency decrease in the MAM (Δ MAM = -0.17°C) of 2017–2025

Table VI Changes in simulated and projected measures of dispersion in GCM20 seasonal precipitation

Time Period	Statistic	DJF	MAM	JJAS	ON
2008–2016 minus 1981	-1989 (2008-2016 min	us 1990–1998)			
ΔF	P10 (mm/day)	0.1 (0)	0 (0)	0 (0)	0 (0)
ΔF	P50 (mm/day)	0.1 (-0.1)	0.1 (-0.6)	1.1 (1.2)	-0.1 (-0.2)
ΔF	P90 (mm/day)	-1.0 (-2.9)	0.1 (-3.4)	5.5 (9)	0.7 (0.1)
ΔM	lean (mm/day)	-0.2 (-0.9)	0 (-1.3)	2.1 (3.3)	0.4 (0.1)
Δ	SD (mm/day)	-0.8 (-1.7)	-0.5 (-2.1)	2.9 (5.4)	1.5 (1)
Δ	Skewness	0 (0.5)	-1.0 (-0.3)	-0.1 (0.1)	1.7 (1.3)
	Δ Kurtosis	4.1 (10.8)	-12.0 (-3.1)	-0.8 (0.6)	36 (27)
2017-2025 minus 1981	-1989 (2017-2025 min	us 1990–1998)			
ΔF	P10 (mm/day)	0.1 (0.1)	0 (0)	0 (0)	0 (0)
ΔF	P50 (mm/day)	0.6 (0.3)	0.5 (-0.2)	0.9 (1.1)	0.1 (0)
ΔF	P90 (mm/day)	0.9 (-1.1)	1.9 (-1.6)	7.1 (10.6)	2.5 (2)
ΔΝ	lean (mm/day)	0.5 (-0.2)	0.7 (-0.6)	2.7 (3.9)	0.8 (0.6)
Δ	SD (mm/day)	0.1 (-0.8)	0.4 (-1.2)	4.9 (7.4)	1.8 (1.3)
Δ	Skewness	-0.2 (0.3)	-1.2 (-0.5)	0.4 (0.6)	0.1 (-0.4)
	Δ Kurtosis	0.1 (6.9)	-16.0 (-7.1)	5.6 (6.9)	0.8 (-8.2)
2081-2089 minus 1981	-1989 (2081-2089 min	us 1990–1998)			
ΔF	P10 (mm/day)	0.1 (0.1)	0 (0)	0 (0)	0 (0)
ΔF	P50 (mm/day)	1.1 (0.8)	0.3 (-0.3)	0.6 (0.8)	0.4 (0.3)
ΔF	P90 (mm/day)	8.9 (7)	2.2 (-1.4)	2.7 (6.2)	3.1 (2.6)
ΔΝ	lean (mm/day)	3.3 (2.7)	0.9 (-0.4)	1.1 (2.2)	1.2 (1)
Δ	SD (mm/day)	6.1 (5.3)	2.1 (0.5)	1.2 (3.6)	3.2 (2.7)
Δ	Skewness	0.6 (1.1)	3.6 (4.3)	-0.1 (0.1)	7.6 (7.2)
	Δ Kurtosis	7 (13.8)	101.1 (110)	0.6 (2)	331.6 (322.6)
2090-2098 minus 1981	-1989 (2090-2098 min	us 1990–1998)			
ΔF	P10 (mm/day)	0 (0)	0 (0)	0 (0)	0 (0)
ΔF	P50 (mm/day)	-0.2 (-0.4)	0.7 (0)	1.4 (1.5)	0.4 (0.3)
ΔF	P90 (mm/day)	-0.8 (-2.7)	2.5 (-1.0)	6.1 (9.7)	3.9 (3.4)
ΔN	lean (mm/day)	-0.2 (-0.8)	1 (-0.3)	2.4 (3.6)	1.5 (1.2)
Δ	SD (mm/day)	0.2 (-0.7)	0.9 (-0.6)	3 (5.4)	3.2 (2.7)
Δ	Skewness	1.3 (1.7)	-0.4 (0.3)	-0.1 (0.1)	2.5 (2.1)
	∆ Kurtosis	18.5 (25.2)	-0.3 (8.5)	1.6 (3)	82.8 (73.8)

Table VII Changes in simulated and projected measures of dispersion in RegCM4.3 seasonal temperature

Time Period	Statistic	DJF	MAM	JJAS	ON
2008–2016	6 minus 1981–1989 (2	008–2016 minus 1990	-1998)		
	Δ P10 (°C)	18.2 (18.1)	14.7 (14.6)	16.4 (17.3)	17.5 (17.8)
	Δ P50 (°C)	5.5 (5.3)	2.8 (2.7)	-0.3 (0.2)	5.7 (5.7)
	Δ P90 (°C)	5.2 (4.7)	2.2 (1.2)	-1.1 (-0.8)	3.3 (4)
	Δ Mean (°C)	7.9 (7.6)	5.2 (5)	2.5 (2.9)	7.4 (7.6)
	Δ SD (°C)	-4.0 (-4.1)	-4.1 (-4.5)	-5.1 (-5.1)	-4.5 (-4.4)
	∆ Skewness	0.2 (0.1)	0.3 (0.3)	0.3 (0.3)	0.2 (0.3)
	∆ Kurtosis	0.5 (0.5)	-0.1 (0.1)	0.1 (0.2)	0.1 (0.1)
2017-2025	5 minus 1981–1989 (2	017-2025 minus 1990	- 1998)		
	Δ P10 (°C)	18.4 (18.3)	14.1 (14)	16.2 (17.1)	17.3 (17.5)
	Δ P50 (°C)	6 (5.7)	2.7 (2.6)	-0.3 (0.2)	5.4 (5.4)
	Δ P90 (°C)	5.8 (5.3)	2 (1)	-0.8 (-0.5)	3.2 (3.9)
	Δ Mean (°C)	8.3 (8)	4.9 (4.7)	2.6 (3)	7.3 (7.5)
	Δ SD (°C)	-3.9 (-4.0)	-3.9 (-4.3)	-5.0 (-5.0)	-4.5 (-4.3)
	∆ Skewness	0.2 (0.2)	0.3 (0.2)	0.4 (0.4)	0.2 (0.3)
	∆ Kurtosis	0.4 (0.4)	0 (0.1)	0 (0)	0.1 (0)
2081-2089	9 minus 1981–1989 (2	081–2089 minus 1990	- 1998)		
	Δ P10 (°C)	18.9 (18.8)	14.8 (14.7)	17 (17.9)	18.3 (18.6)
	Δ P50 (°C)	8.3 (8)	4.7 (4.5)	2.1 (2.6)	8.3 (8.3)
	Δ P90 (°C)	9.1 (8.6)	5.3 (4.3)	1.7 (2)	6.8 (7.5)
	Δ Mean (°C)	10.6 (10.2)	6.9 (6.7)	4.4 (4.9)	9.9 (10.1)
	Δ SD (°C)	-2.9 (-3.0)	-3.1 (-3.5)	-4.3 (-4.3)	-3.5 (-3.3)
	∆ Skewness	0.2 (0.2)	0.4 (0.3)	0.3 (0.3)	0.2 (0.2)

Δ Kurtosis	0.3 (0.3)	-0.3 (-0.1)	-0.1 (0)	0.1 (0)
2090-2098 minus 1981-1989 (20	090–2098 minus 1990)–1998)		
Δ P10 (°C)	19 (18.9)	14.7 (14.6)	16.8 (17.7)	18.1 (18.4)
Δ P50 (°C)	8.2 (7.9)	5 (4.9)	2 (2.5)	8.2 (8.2)
Δ P90 (°C)	9.2 (8.7)	5 (4)	1.7 (2)	6.5 (7.2)
Δ Mean (°C)	10.5 (10.2)	6.9 (6.7)	4.5 (4.9)	9.7 (9.9)
Δ SD (°C)	-2.9 (-3.0)	-3.0 (-3.4)	-4.2 (-4.3)	-3.5 (-3.4)
∆ Skewness	0.3 (0.2)	0.3 (0.2)	0.3 (0.3)	0.2 (0.2)
Δ Kurtosis	0.2 (0.2)	-0.1 (0)	-0.1 (-0.1)	0.1 (0)

Table VIII Changes in simulated and projected measures of dispersion in RegCM4.3 seasonal precipitation

Time Period	Statistic	DJF	MAM	JJAS	ON
2008–201	16 minus 1981-1989 (200	8–2016 minus 1990–19	998)		
	Δ P10 (mm/day)	0.6 (0.6)	0.5 (0.5)	0.7 (0.7)	0.4 (0.4)
	Δ P50 (mm/day)	3.5 (3.5)	3.7 (3.7)	5.3 (5.3)	3.6 (3.5)
	Δ P90 (mm/day)	19.9 (20)	19.5 (19.8)	29.9 (29.2)	18.2 (18.5)
	Δ Mean (mm/day)	8.2 (8.2)	8 (8.1)	11.5 (11.1)	8.3 (8.2)
	Δ SD (mm/day)	13.6 (13.5)	13.3 (13.4)	16.7 (15.6)	15.4 (14.7)
	∆ Skewness	-0.1 (-1.2)	0.5 (-0.3)	-2.5 (-3.3)	-0.3 (-2.1)
	∆ Kurtosis	-1.6 (-24.0)	7.5 (-12.5)	-40.9 (-61.7)	-15.9 (-54.3)
2017-202	25 minus 1981-1989 (201	7–2025 minus 1990–19	998)		
	Δ P10 (mm/day)	0.7 (0.7)	0.7 (0.7)	0.8 (0.8)	0.4 (0.4)
	Δ P50 (mm/day)	4.5 (4.5)	3.7 (3.8)	5.3 (5.3)	3.7 (3.7)
	Δ P90 (mm/day)	23.5 (23.6)	22.8 (23.1)	26.1 (25.5)	19.7 (19.9)
	Δ Mean (mm/day)	9.6 (9.6)	8.3 (8.5)	10.9 (10.5)	8.2 (8.1)
	Δ SD (mm/day)	15.4 (15.3)	12.3 (12.5)	16 (14.9)	13.7 (13)
	∆ Skewness	0 (-1.1)	0 (-0.9)	-2.0 (-2.7)	-0.6 (-2.4)
	∆ Kurtosis	-1.4 (-23.8)	4.6 (-15.3)	-34.4 (-55.2)	-17.3 (-55.7)
2081-208	39 minus 1981–1989 (208	1-2089 minus 1990-19	998)		
	Δ P10 (mm/day)	0.7 (0.7)	0.7 (0.7)	0.8 (0.8)	0.5 (0.5)
	Δ P50 (mm/day)	3.7 (3.7)	3.8 (3.8)	4.9 (4.8)	3.2 (3.1)
	Δ P90 (mm/day)	17 (17.1)	14.6 (14.9)	25.2 (24.6)	14.4 (14.7)
	∆ Mean (mm/day)	6.6 (6.6)	6.2 (6.3)	10 (9.6)	5.7 (5.6)
	Δ SD (mm/day)	7.7 (7.6)	6.9 (7.1)	13.5 (12.3)	7.2 (6.6)
	∆ Skewness	-1.8 (-2.9)	-1.2 (-2.0)	-2.8 (-3.5)	-1.8 (-3.6)
	∆ Kurtosis	-19.8 (-42.2)	-10.5 (-30.5)	-42.6 (-63.4)	-30.8 (-69.1)
2090-209	98 minus 1981–1989 (209	0–2098 minus 1990–19	998)		
	Δ P10 (mm/day)	0.9 (0.9)	0.8 (0.8)	0.9 (0.9)	0.6 (0.6)
	Δ P50 (mm/day)	4.8 (4.8)	3.9 (3.9)	5 (5)	4 (4)
	Δ P90 (mm/day)	19.4 (19.5)	16.5 (16.8)	21.9 (21.2)	18.8 (19)
	Δ Mean (mm/day)	8.4 (8.4)	7 (7.2)	9.4 (9)	7.5 (7.4)
	Δ SD (mm/day)	10.9 (10.8)	8.8 (8.9)	12.6 (11.5)	9.9 (9.2)
	∆ Skewness	-0.7 (-1.8)	-1.1 (-1.9)	-2.1 (-2.8)	-1.6 (-3.4)
	∆ Kurtosis	-9.1 (-31.5)	-11.7 (-31.7)	-33.7 (-54.5)	-27.8 (-66.2)

projection period which indicates a relative decrease in the number of cold MAM days in the immediate future period. Furthermore, both GCM20 and RegCM4.3 suggest higher occurrences of MAM warm days in the 2080–2098 projection period. AgMERRA displays that relative frequency of cold days had increased in the 1990–1998 JJAS due to positive changes in P10. Both GCM20 and RegCM4.3 suggest a relative drop in P90 suggesting a relative cooling in warm JJAS days of the 2008–2025 projection period. AgMERRA displays relative frequency drop in all P10, P50 and P90 of the 1980–1998 ON. GCM20 indicates a drop in P10 suggesting lower frequency of cold ON days in the 2008–2016 projection period. RegCM4.3 suggests ON warm days to recur with higher frequencies in 2017–2025 projection period.

In mean precipitation regime, AgMERRA displays a relative frequency decrease in the mean and an increase of 30 mm/day mean precipitation events in 1990–1998 baseline period of DJF. Both GCM20

and RegCM4.3 suggests a relative frequency increase in 5 mm/day to 35 mm/day mean precipitation occurrences for 2008–2025 projection period. RegCM4.3 further suggests a P10 frequency increase (Δ DJF = 0.9 mm/day) in the 2081–2089 projection period. For the MAM mean precipitation, AgMERRA displays a relative increase in all computed percentiles with relatively higher variability in the 1990–1998 baseline period. As per GCM20 and RegCM4.3 results, MAM mean precipitation suggests a relative increase in 10 mm/day to 30 mm/day mean precipitation occurrences in 2017–2025 and 2081–2089 projection periods. For the JJAS mean precipitation, AgMERRA displays relative decrease in the P90 (Δ JJAS = –1.8 mm/day) of the 1990–1998 baseline period. On the other hand, GCM20 in 2008–2016 projection period suggests a relative increase in 45 mm/day mean precipitation occurrences with simultaneous increase of P90 in the JJAS. RegCM4.3 also suggests a substantial rise in P90 (Δ JJAS = 29.9 mm/day) in the

2008–2016 projection period. Finally, for the ON mean precipitation, AgMERRA displays higher variability with simultaneous rise in P10, P50 and P90 mean precipitation occurrences that resulted in higher frequencies of 10 mm/day to 15 mm/day mean precipitation events in 1990–1998 baseline period. GCM20 suggests higher variability and higher mean precipitation occurrences of 5 mm/day to 30 mm/day with simultaneous rise in P90 of the ON of 2017–2025 projection period. RegCM4.3 also suggests higher occurrences of 5 mm/day to 30 mm/day mean precipitation events in the 2008–2025 and 2080–2098 projection periods of the ON.

Acknowledgements

The authors thank Goddard Institute for Space Studies (GISS NASA) for providing reanalysis datasets for this research work. Special regards to Data Integration and Analysis System (DIAS) for providing Global Circulation Model (GCM) data. The authors are grateful to International Center for Theoretical Physics (ICTP) for providing output of Regional Climate Model (RCM) simulated over Pakistan. The authors thank Pakistan Meteorological Department (PMD) for providing technical resources for this study.

REFERENCES

- Athar H. 2012. Decadal variability of the observed daily temperature in Saudi Arabia during 1979–2008. Atmospheric Science Letters 13: 244–249.
- Athar H. 2013. Seasonal variability of the observed and the projected daily temperatures in northern Saudi Arabia. *Climatic Change* 119: 333–344.
- Burhan A. 2016. An analysis of climate change in Pakistan. MS Thesis, Department of Meteorology, COMSATS Institute of Information Technology Islamabad, Pakistan.
- Chen J, Brissette FP, Leconte R. 2011. Uncertainty of downscaling method in quantifying the impact of climate change on hydrology. *Journal of Hydrology* 401: 190–202.
- Dimri AP, Niyogi D, Barros AP, Ridley J, Mohanty UC, Yasunari T, Sikka DR. 2015. Western Disturbances: A review. Reviews of Geophysics 53: 225–246.
- Donat MG, Alexander LV. 2012. The shifting probability distribution of global daytime and night–time temperatures. *Geophysical Research Letters* 39: 1–5.
- Fowler HJ, Blenkinsop S, Tebaldi C. 2007. Linking climate change modelling to impacts studies: recent advances in downscaling techniques for hydrological modelling. *International Journal of Climatology* 27: 1547–1578.
- Franco R, Coppola E, Giorgi F, Graef F, Pavia EG. 2013. Assessment of RegCM4 simulated inter–annual variability and daily–scale statistics of temperature and precipitation over Mexico. *Climate Dynamics* 42: 629–647.
- Giorgi F, Coppola E, Solmon F, Mariotti L, Sylla MB, Bi X, Elguindi N, Diro GT, Nair V, Giuliani G, Turuncoglu UU, Cozzini S, Güttler I, O'Brien TA, Tawfik AB, Shalaby A, Zakey AS, Steiner AL, Stordal F, Sloan LC, Brankovic C. 2012. RegCM4: Model description and preliminary tests over multiple CORDEX domains. *Climate Research* 52: 7–29.
- Gu H, Wang G, Yu Z, Mei R. 2012. Assessing future climate changes and extreme indicators in east and south Asia using the RegCM4 regional climate model. Climatic Change 114: 301–317.
- Immerzeel WW, Van Beek LPH, Konz M, Shrestha AB, Bierkens MFP, 2012: Hydrological response to climate change in a glacierized catchment in the Himalayas. *Climatic Change* 10: 721–736.
- Kitoh A, Yatagai A, Alpert P. 2008. First super-high-resolution model projection that the ancient "Fertile Crescent" will disappear in this century. *Hydrological Research Letters* 2: 1–4.

- Kitoh A, Ose T, Kurihara K, Kusunoki S, Sugi M. 2009. Projection of changes in future weather extremes using super–high–resolution global and regional atmospheric models in the KAKUSHIN Program: Results of preliminary experiments. *Hydrological Research Letters* 3: 49–53.
- Knutti R. 2008. Should we believe model predictions of future climate change? Philosophical Transactions. Series A, Mathematical, Physical, and Engineering Sciences 366: 4647–4664.
- Kundu A, Denis DM, Patel NR. 2015. Evaluation of the meteorological drought over the Bundelkhand region using geo-spatial techniques. Climate Change, 1(4), 418-424
- Kusunoki S, Yoshimura J, Yoshimura H, Noda A. 2006. Change of baiu rain band in global warming projection by an atmospheric general circulation model with a 20–km grid size. *Journal of the Meteorological Society of Japan* 84: 581–611.
- Larson JW. 2012. Visualizing climate variability with time-dependent probability density functions, detecting it using information theory. Procedia Computer Science 9: 917–926.
- Michczynska DJ, Pazdur A. 2004. Shape analysis of cumulative probability density function of radiocarbon dates set in the study of climate change in the late glacial and holocene. *Radiocarbon* 46: 733–744.
- Minville M, Brissette F, Leconte R. 2008. Uncertainty of the impact of climate change on the hydrology of a nordic watershed. *Journal of Hydrology* 358: 70–83.
- Mizuta R, Hiromasa Y, Hiroyuki M, Mio M, Hirokazu E, Tomoaki O, Kenji K, Masahiro H, Masato S, Seiji Y, Shoji K and Akio K.2012.
 Climate Simulations Using MRI–AGCM3.2 with 20–km Grid. *Journal* of the Meteorological Society of Japan 90A: 233–258.
- Ozturk T, Altinsoy H, Türkeş M, Kurnaz M. 2012. Simulation of temperature and precipitation climatology for the Central Asia CORDEX domain using RegCM4.0. Climate Research 52: 63–76.
- Rasmussen KL, Hill A,Toma VE, Zuluaga MD, Webster PJ, Houze RA. 2015. Multiscale analysis of three consecutive years of anomalous flooding in Pakistan. *Quarterly Journal of Royal Meteorological Society* 141: 1259–1276.
- Robert W. 2014. Statistical downscaling of probability density function of daily precipitation on the Polish coast PilarskiMichałMiętusMirosław, Meteorology, Hydrology and Water Management, Research and Operational Applications 2: 27–36.
- Ruane A, Goldberg R, Chryssanthacopoulos J. 2014. AgMIP climate forcing datasets for agricultural modeling: Merged datas for gap-filling and historical climate series estimation. Agricultural and Forest Meteorology 200: 233–248.
- Salathe Jr. EP. 2004: Methods for selecting and downscaling simulations of future global climate with application to hydrologic modelling. *International Journal of Climatology* 25: 419–436.
- Shamshad KM. 1988. The meteorology of Pakistan: Climate and weather of Pakistan, 1st ed, Royal Book Company, Karachi, Pakistan.
- 27. Tisseuil C, Vrac M, Lek S, Wade AJ. 2010. Statistical downscaling of river flows. *Journal of Hydrology* 385: 279–291.
- Watterson IG. 2008. Calculation of probability density functions for temperature and precipitation change under global warming. *Journal* of *Geophysical Research* 113: 1–13.
- 29. Wand MP, Jones MC. (1995). Kernel Smoothing. *Chapman and Hall, London.*
- Wang B. 2006. The Asian Monsoon. Springer/Praxis Publishing Co., New York
- 31. Winkler JA, Guentchev GS, Liszewska M, Tan P. 2011. Climate scenario development and applications for local/regional climate change impact assessments: An overview for the non–climate scientist part II: considerations when using climate change scenarios. *Geography Compass* 6: 301–328.
- Wilks DS. 2011. Statistical Methods in the Atmospheric Sciences, Third edn. Elsevier Publishers: New York.

RESEARCH ARTICLE

- Wood A, Leung LR, Sridhar V, Lettenmaier DP. 2004: Hydrologic implications of dynamical and statistical approaches to downscaling climate model outputs. *Climatic Change* 62, 189–216.
- 34. Yatagai A, Xie P, Kitoh A. 2005. Utilization of a new gauge—based daily precipitation dataset over monsoon Asia for validation of the daily precipitation climatology simulated by the MRI/JMA 20–km mesh AGCM. Scientific Online Letters on the Atmosphere 1: 193– 196.

Article Keywords

AgMERRA; GCM20; RegCM4.3; PDFs; climate change, Pakistan

Article History

Received: 22 September 2018 Accepted: 08 November 2018 Published: January - March 2019

Citation

Burhan A, Athar H. PDF based seasonal changes in AgMERRA observations and GCM20 and RegCM4.3 projections over Pakistan Region. *Climate Change*, 2019, 5(17), 68-81

Publication License



© The Author(s) 2019. Open Access. This article is licensed

under a Creative Commons Attribution License 4.0 (CC BY 4.0).

General Note

Article is recommended to print as color version in recycled paper. Save Trees, Save Climate.